TU Delft

Delft University of Technology

Document Version
Accepted author manuscript

Citation (APA)
Owen, C., & Hendrikse, H. (2018). Ice-induced vibrations of model structures with various dynamic properties. In *Proceedings of the 24th IAHR International Symposium on Ice: 4-10 June 2018, Far Eastern Federal University, Vladivostok, Russia* (pp. 376-386).

Important note
To cite this publication, please use the final published version (if applicable).
Please check the document version above.

Copyright
In case the licence states “Dutch Copyright Act (Article 25fa)”, this publication was made available Green Open Access via the TU Delft Institutional Repository pursuant to Dutch Copyright Act (Article 25fa, the Taverne amendment). This provision does not affect copyright ownership.
Unless copyright is transferred by contract or statute, it remains with the copyright holder.

Sharing and reuse
Other than for strictly personal use, it is not permitted to download, forward or distribute the text or part of it, without the consent of the author(s) and/or copyright holder(s), unless the work is under an open content license such as Creative Commons.

Takedown policy
Please contact us and provide details if you believe this document breaches copyrights.
We will remove access to the work immediately and investigate your claim.

This work is downloaded from Delft University of Technology.

International Association for Hydro-Environment Engineering and Research
Supported by Spain Water and IWHR, China

24th IAHR International Symposium on Ice
Vladivostok, Russia, June 4 to 9, 2018

Ice-Induced Vibrations of Model Structures with Various Dynamic Properties

Cody C. Owen, Hayo Hendrikse
Department of Hydraulic Engineering at Delft University of Technology
Building 23, Stevinweg 1, 2628CN Delft, the Netherlands
C.C.Owen@tudelft.nl, H.Hendrikse@tudelft.nl

For the design of offshore structures in regions with ice-infested waters, the prediction of interaction between floating level ice and the support structure is essential. If the structure is vertically sided at the ice-structure interface and certain ice and structural conditions exist, then the phenomenon known as ice-induced vibrations can develop. Recently, an ice-structure interaction model has been developed and validation has been attempted based on dedicated experiments. This study extends the validation by investigating the capabilities of the analytical model in predicting the indentation speed range for the frequency lock-in regime of ice-induced vibrations with various input parameters. Implementation of these various input parameters seeks to address the challenge of adapting the analytical model from the reference input parameters to scenarios with other structural properties. Using these various input parameters, the analytical model can demonstrate accurate prediction of frequency lock-in vibrations as observed in the experiments when the mean global ice load in crushing is properly estimated. For the cases when the mean global ice load was not properly estimated, either unsuitable scaling between input parameters, undesirable behavior of the model ice during the experiments, or a combination thereof may be the cause. Overall, this study serves to establish the range of applicability for the analytical model in terms of accurate prediction of frequency lock-in vibrations between model ice and various structures and discusses the sensitivity of the analytical model with respect to the input parameters. This study is an important step towards application of the analytical model for full-scale scenarios.

1. Introduction

For the design of offshore structures in regions with ice-infested waters, the prediction of interaction between floating level ice and the support structure is essential. If the structure is vertically sided at the ice-structure interface and certain ice and structural conditions exist, then the phenomenon known as ice-induced vibrations can develop. Some ice-structure interaction models have attempted to predict ice-induced vibrations, but issues have arisen regarding their range of applicability for various dynamic properties of the structures (Jeong et al., 2010; Kärnä et al., 2013; Muhonen, 1996). Recently, a phenomenological model has been developed and validation has been attempted based on dedicated experiments (Hendrikse et al., 2018). These experiments belong to an extensive model-scale testing campaign as part of the Ice-induced Vibrations of Offshore Structures (IVOS) project and were conducted by the Hamburg Ship Model Basin (HSVA). From the validation attempt of the analytical model, input parameters to define the model ice behavior were derived with a reference structure.

With the previously determined input parameters, experiments from the IVOS project with similar ice conditions but with structures that differ from the reference structure are simulated to investigate the capabilities of the analytical model. This validation focuses on assessing the predictive capabilities of the analytical model in determining the indentation speed range within which the frequency lock-in regime of ice-induced vibrations develops. The working principle is that if the mean global ice load magnitude is properly estimated in the analytical model, then the frequency lock-in regime should be predicted correctly regardless of the structural properties. Determining an accurate global ice load level is dependent on the scaling from the predetermined reference parameters and to other parameters. In this study, it is proven that proper estimation of the global ice load by the analytical model can produce results that correspond well with experimental observations in the frequency lock-in regime of ice-induced vibrations. Furthermore, scaling of the reference parameters to different ice conditions as input to the analytical model for prediction of the frequency lock-in regime is attempted and the results are expounded.

2. IVOS Experimental Campaign

The Phase 1 and Phase 2 experiments of the IVOS campaign with model ice were conducted between 2015 and 2016 by HSVA in their Large Ice Basin (Ziemer et al., 2017). Model structures with various configurations of size, cross-sectional geometry (shape) at the ice-structure interface, fundamental natural frequency, and stiffness were utilized for indentation tests in model ice over a range of indentation speeds (Hinse et al., 2017). Figure 1 illustrates the test apparatus and size and shape of the model structures of the IVOS experiments that are specifically chosen for this study. Detailed ice properties were recorded for each of the experiments and the pertinent measurements, and their use, are elaborated in Section 5.

3. Analytical Model

The analytical model used for this study is described in Hendrikse et al. (2018) and further explanation of the physical basis and derivation is given by Hendrikse (2017). The reference parameters to define the HSVA model ice behavior have been determined in Hendrikse et al. (2018) and are shown in Table 1.

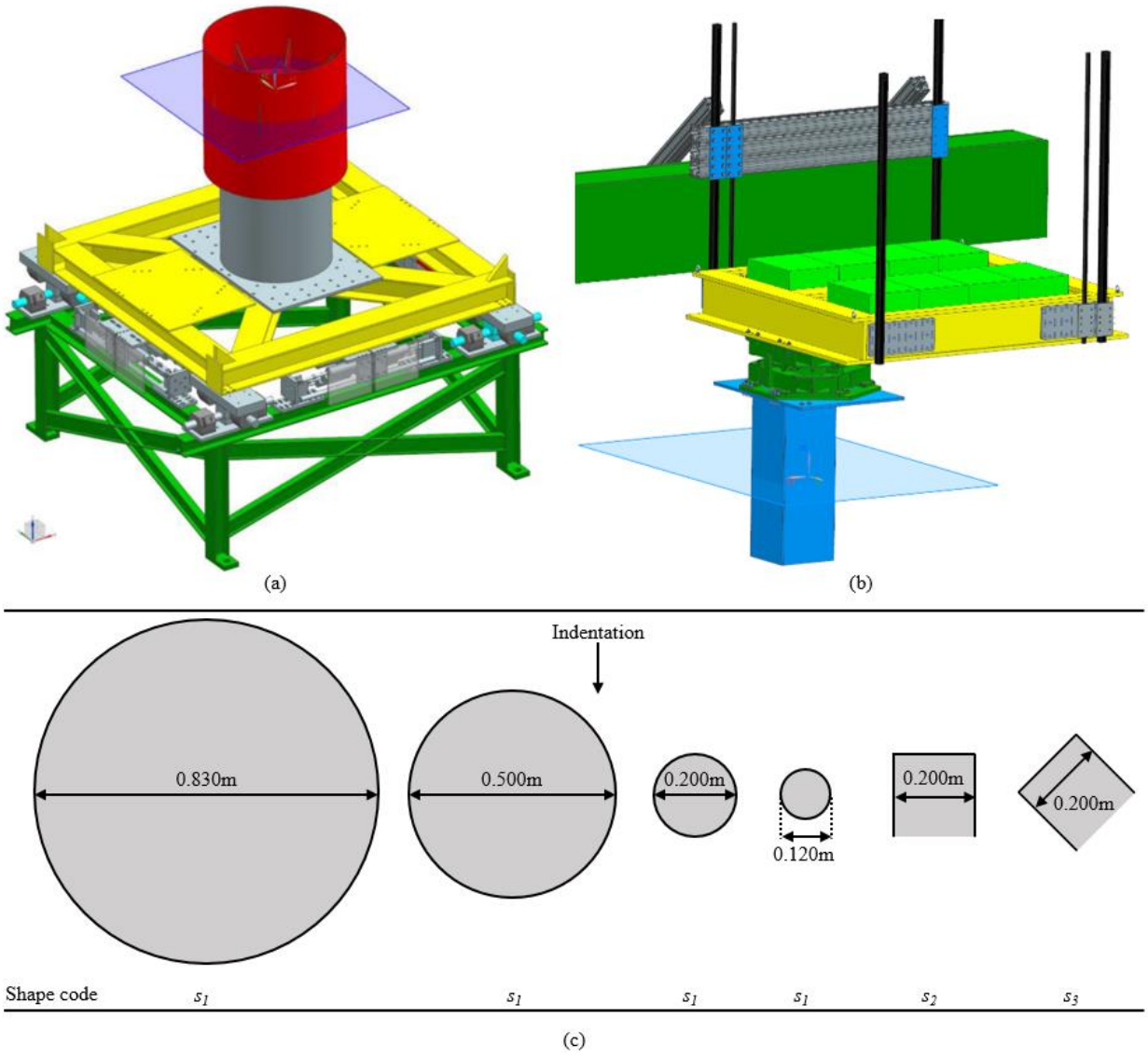

Fig. 1. Schematics of the test apparatus and size and shape of select model structures from the IVOS experiments, of which (a) is the Phase 1 test apparatus; (b) is the Phase 2 test apparatus; and (c) is the schematic of model structure cross-sections with shape and shape code, size, and orientation of indentation (Hinse et al., 2017; Ziemer et al., 2017).

Table 1. Reference input parameters from HSVA model ice for the analytical model derived from the indentation experiment with the rigid reference structure (Hendrikse et al., 2018).

$K_{2,ref}$ [N m^{-1}]	$C_{2,ref}$ [N^3 m^{-1} s]	$K_{1,ref}$ [N m^{-1}]	$C_{1,ref}$ [N m^{-1} s]	N_{ref} [-]	$r_{max,ref}$ [m]	$\delta_{f,ref}$ [m]
$5.091 \cdot 10^4$	$1.05 \cdot 10^9$	$5.372 \cdot 10^3$	$1.7021 \cdot 10^4$	39	$2.9 \cdot 10^{-3}$	$2 \cdot 10^{-3}$

4. Scaling Approach

The reference input parameters with subscript *ref* in Table 1 are the result of specific ice conditions, the HSVA model ice in this case, and a structure with distinct size and shape. For the different ice conditions observed during the experiments and for the shapes of the various model structures, the reference input parameters are scaled according to Hendrikse et al. (2018) as follows:

$$
\begin{aligned}
N &= N_{ref}\,(d / d_{ref}) \\
K_2 &= K_{2,ref}\,(\sigma / \sigma_{ref})\,(h / h_{ref})\,s_s(s,s_{ref}) \\
C_2 &= C_{2,ref}\,(\sigma / \sigma_{ref})\,(h / h_{ref})\,s_s(s,s_{ref}) \\
K_1 &= K_{1,ref}\,(\sigma / \sigma_{ref})\,(h / h_{ref})\,s_s(s,s_{ref}) \\
C_1 &= C_{1,ref}\,(\sigma / \sigma_{ref})\,(h / h_{ref})\,s_s(s,s_{ref}) \\
r_{max} &= r_{max,ref} \\
\delta_f &= \delta_{f,ref}
\end{aligned}
\qquad \textbf{[1]}
$$

which assume a linear dependence of the mean global ice load in crushing on structural width d, compressive ice strength σ, ice thickness h, and shape factor $s_s(s,s_{ref})$. Note that the variable for the shape factor from Hendrikse et al. (2018) is changed from $f_s(s,s_{ref})$ to $s_s(s,s_{ref})$ for clarity in this article. It has been observed experimentally and analytically that indentation shape affects the global ice load level when comparing structures of similar size (Korzhavin, 1971; Owen, 2017). As a preliminary method to substantiate the effect of load level on specific indentation shapes, an elastic-plastic indentation model with different shapes of indenters is employed (Yu et al., 1996). The rigid model structure utilized to obtain the reference input parameters had a square cross-section with side-first indentation in the model ice sheet; therefore, the reference shape s_{ref} is defined as rectangular. The shape s of indentation of the structures considered in this study are circular s_1, rectangular s_2, and triangular s_3. For the shapes that differ from the reference shape, the shape factor $s_s(s,s_{ref})$ is determined by the elastic-plastic indentation model as the ratio between the loads from the shape s and from the reference shape s_{ref} for indenters of equivalent size and for equivalent ice conditions. Based on the model ice properties and the sizes and shapes of the model structures, the indentation model predicts shape factors $s_s(s,s_{ref})$ for the circular and triangular shapes of roughly 0.8 and 0.7, respectively, when compared to a rectangular shape with shape factor $s_s(s,s_{ref})$ of 1.0. These results generally agree with the findings by Korzhavin (1971) and Owen (2017). These shape factors are selected as inputs to the numerical model as shown in Equation 1 and implemented in Section 5.

5. Simulation Parameters

The input parameters to the analytical model for the simulations are shown in Table 2. Each structure is simulated as a single-degree-of-freedom oscillator, which follows the design objective of the test apparatus from the IVOS experiments. The fundamental natural frequency f_s and stiffness K_s of each model structure were provided by HSVA (Hinse et al., 2017). The damping as a ratio of critical damping ζ_s was determined by logarithmic decrement from a relaxation test for each of the structures (Owen, 2017). It was observed during the experiments that the properties of the model ice varied spatially throughout the basin and among the different ice sheets. To capture effects of the variation in ice properties on the ice-structure interaction, a range of ice thickness h and compressive strength σ are considered for the simulations. Each

structure is subjected to three different ice condition cases in the simulations. In the first case, the mean ice thickness and mean compressive ice strength as determined from the corresponding experiments are simulated. The second case considers the minimum ice thickness observed during any of the corresponding experiments and 10% less than the minimum compressive ice strength computed from any of the corresponding experiments. Finally, the third case considers the maximum ice thickness observed during any of the corresponding experiments and 10% greater than the maximum compressive ice strength computed from any of the corresponding experiments. As suggested by HSVA, the 10% variation for the compressive ice strength is included because the compressive ice strength values were computed based on only one sample location for each of the ice sheets. The mean load adjustment factor is disregarded for the first set of simulations and is addressed in Section 6.

For each trial, simulations are performed from an indentation speed of 0.003 m s^{-1} to 0.150 m s^{-1} with increments of 0.001 m s^{-1} as performed in the experiments. The initial conditions of the structure for each simulation are defined as the final conditions of the structure from the simulation of the previous indentation speed. This is chosen to recreate the stepwise increase in consecutive indentation speeds as done in the experiments. Each simulation is executed for 20 seconds and the final 10 seconds are exclusively considered for statistical analysis of the steady-state response.

6. Comparison of Experiments and Simulations

To compare the experiments and simulations regarding the frequency lock-in regime of ice-induced vibrations, criteria are defined to identify this particular regime. As a basic criterion, the frequency lock-in regime of ice-induced vibrations can be defined by the ratio of the maximum structural velocity and the indentation speed, known as β, between 1.0 and 1.5 (Hendrikse, 2017). Following this definition, the experiments and simulations are examined for recurring instances when β is between 1.0 and 1.5, when the structural response is quasi-sinusoidal near the fundamental natural frequency, and when the global ice load periodically is amplified ensuing the time when the relative velocity between ice and structure is low. For this study, adequate development of frequency lock-in vibrations is achieved for the experiments when the aforementioned criteria are met for at least three consecutive cycles. The choice of at least three consecutive cycles is made in an attempt to inclusively identify frequency lock-in vibrations as a result of nearly constant ice conditions. But because the ice conditions were known to vary substantially for a given indentation speed, requiring more consecutive cycles could potentially exclude indentation speeds during which frequency lock-in vibrations develop. The simulated results are considered frequency lock-in vibrations when the aforementioned criteria are met for a majority of the time history.

Figure 2 shows the comparison between the experimental observations of frequency lock-in vibrations and the predicted lower and upper bounds within which the frequency lock-in regime of ice-induced vibrations develops. The predicted bounds for frequency lock-in vibrations are in close agreement with the experimental observations. Frequency lock-in vibrations are observed below the predicted lower bound for most of the experiments, which is explained in Section 7. Not all of the experiments contained an indentation speed resolution required to yield a complete range for the frequency lock-in regime. But for the experiments with sufficient indentation speed resolution, the predicted upper bounds for frequency lock-in vibrations that are higher than

experimentally observed (see trials T6 and T9 in Figure 2) can be explained by an improper estimation of the mean global ice load in crushing. This is further discussed in Section 7.

To quantify the effect of proper estimation of mean global ice load in crushing on the range of indentation speeds during which frequency lock-in vibrations develop, a mean load adjustment is applied as a factor in the same manner as the shape factor (see Table 2). The mean load adjustment factor is determined a posteriori by computing the ratio of the simulated mean load and the experimental mean load in crushing for the highest experimental indentation speed. Applying this factor and repeating the simulations, the simulated bounds for frequency lock-in vibrations generally fit better with the experimental observations (see Figure 3). However, no frequency lock-in vibrations are predicted for trials T2 and T3 in Figure 3 with the mean load adjustment. The mean global ice loads obtained from the experiments corresponding to trials T2 and T3 were highly influenced by flexural behavior of the ice; this is explained in Section 7.

Figure 4 exemplifies the result of proper mean global ice load level estimation in terms of global ice load and structural displacement time traces in the frequency lock-in regime. A low-pass filter with cutoff frequency of 49 Hz was applied to the experimental global ice load signal to attenuate noise from the data acquisition power source, and was applied to the simulated ice load signal for comparative consistency.

7. Discussion

Based on general trends from the experiments, the analytical model can demonstrate accurate prediction of the range of indentation speeds within which frequency lock-in vibrations develop. However, this accurate prediction is predicated on proper estimation of the mean global ice load level by the analytical model. For the mean global ice load level to be properly estimated using the input parameters that differ from the reference parameters, a type of scaling must be applied. Reviewing Figure 2 and Figure 3, it can be deduced that the linear scaling in Equation 1 may not be suitable for the various dynamic properties that differ significantly from the reference parameters. But it is not clear whether the type of scaling or the flexural behavior of the model ice is the cause.

It was observed that the spatial variations in ice conditions were substantial during the IVOS experiments with model ice. These variations in ice conditions mean that, during an experiment, the mean global ice load changed not only with indentation speed but also with the ice properties. The ice conditions, such as ice thickness and uniaxial compressive ice strength, were not reported for the entirety of each ice sheet and thus could not be accurately simulated. Moreover, nearly steady-state ice-structure interaction for statistical analysis cannot be reliably observed during experiments with such large spatial variation in ice conditions. In addition, the flexural behavior of the model ice was such that ice failure in crushing was not always the dominant failure mechanism and, as a result, the mean global ice load differed from the predictions. Out-of-plane, downward bending and failure of the ice sheet was consistently observed in the experiments for the lower indentation speeds, which reduced the mean global ice loads and limited the development of ice-induced vibrations. For example, intermittent crushing vibrations did not properly develop for any of the IVOS experiments because of the flexural behavior of the model ice. In the case of low indentation speeds for the Phase 2 experiments, the

ice bending resulted in conditions suitable for frequency lock-in vibrations. These conditions are not included in the analytical model and therefore would not be predicted.

Table 2. Input parameters to the analytical model for simulation of the IVOS experiments.

Trial name	Shape code	$s_s(s,s_{ref})$ [-]	d [m]	f_s [Hz]	K_s [kN m^{-1}]	ζ_s [%]	h [m]	σ [kPa]	Mean load adjustment factor [-]
T0_0	s_1	0.8	0.830	5.45	2230	1.5	0.048	81	0.28
T0_1							0.044	61	
T0_2							0.052	106	
T1_0	s_1	0.8	0.830	2.65	490	3.0	0.046	98	0.21
T1_1							0.042	58	
T1_2							0.049	131	
T2_0	s_1	0.8	0.500	5.47	2220	2.0	0.031	90	0.24
T2_1							0.026	81	
T2_2							0.034	99	
T3_0	s_1	0.8	0.500	7.60	3020	2.9	0.031	80	0.36
T3_1							0.028	72	
T3_2							0.033	88	
T4_0	s_1	0.8	0.200	5.78	1930	2.4	0.042	97	0.41
T4_1							0.040	87	
T4_2							0.045	107	
T5_0	s_1	0.8	0.500	5.47	2030	1.7	0.043	72	0.32
T5_1							0.040	65	
T5_2							0.047	79	
T6_0	s_1	0.8	0.120	5.40	1935	1.0	0.041	136	1.13
T6_1							0.038	122	
T6_2							0.044	150	
T7_0	s_2	1.0	0.200	4.18	1290	1.8	0.048	125	0.89
T7_1							0.045	104	
T7_2							0.051	160	
T8_0	s_3	0.7	0.283	5.59	1915	2.2	0.044	110	0.55
T8_1							0.040	99	
T8_2							0.047	121	
T9_0	s_2	1.0	0.200	5.4	1950	1.7	0.045	110	0.81
T9_1							0.042	99	
T9_2							0.048	121	

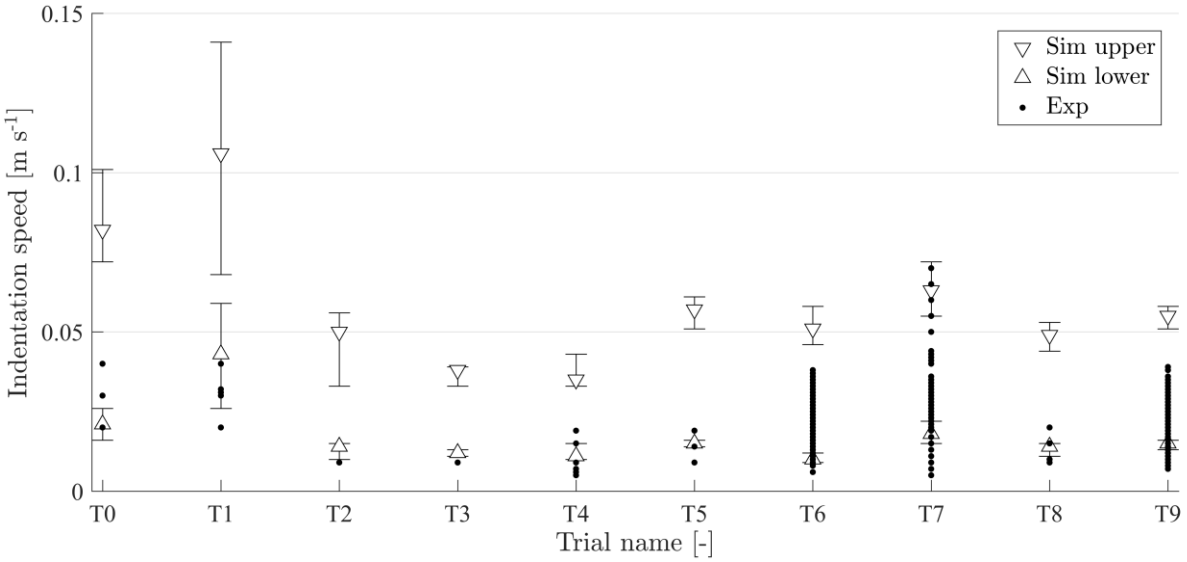

Fig. 2. Comparison of simulated (Sim) lower and upper bounds for frequency lock-in regime and observed (Exp) frequency lock-in vibrations from the experiments. Each simulated bound is represented by a triangle with a higher and lower error bar indicating simulation results from the mean, maximum, and minimum ice condition cases, respectively.

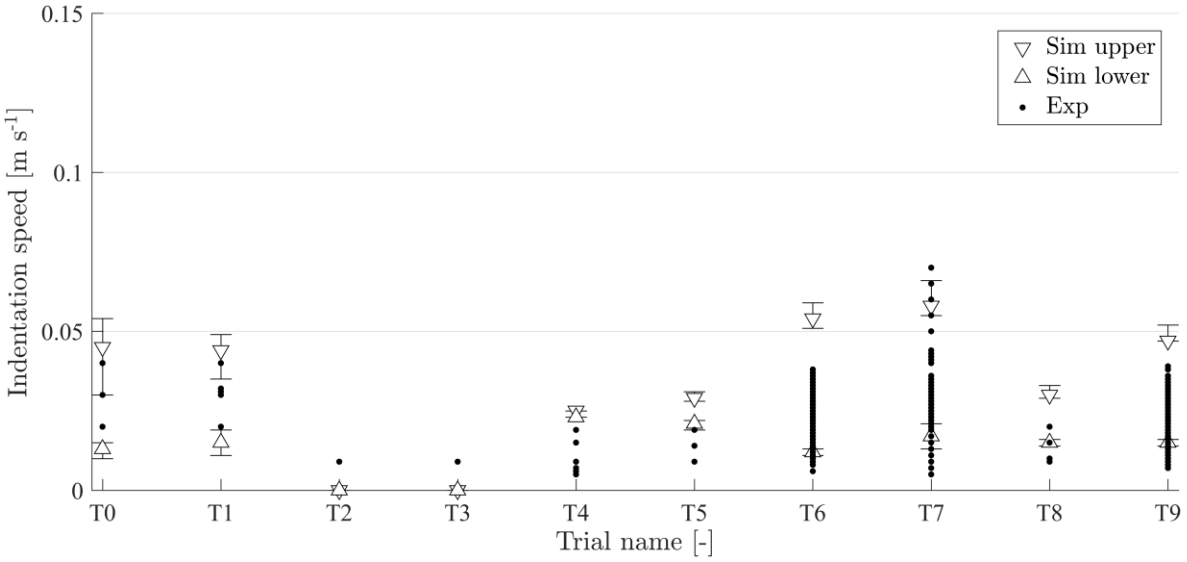

Fig. 3. Comparison of simulated (Sim) lower and upper bounds for frequency lock-in regime with mean load adjustment and observed (Exp) frequency lock-in vibrations from the experiments. Each simulated bound is represented by a triangle with a lower and higher error bar indicating simulation results from the mean, minimum, and maximum ice condition cases, respectively.

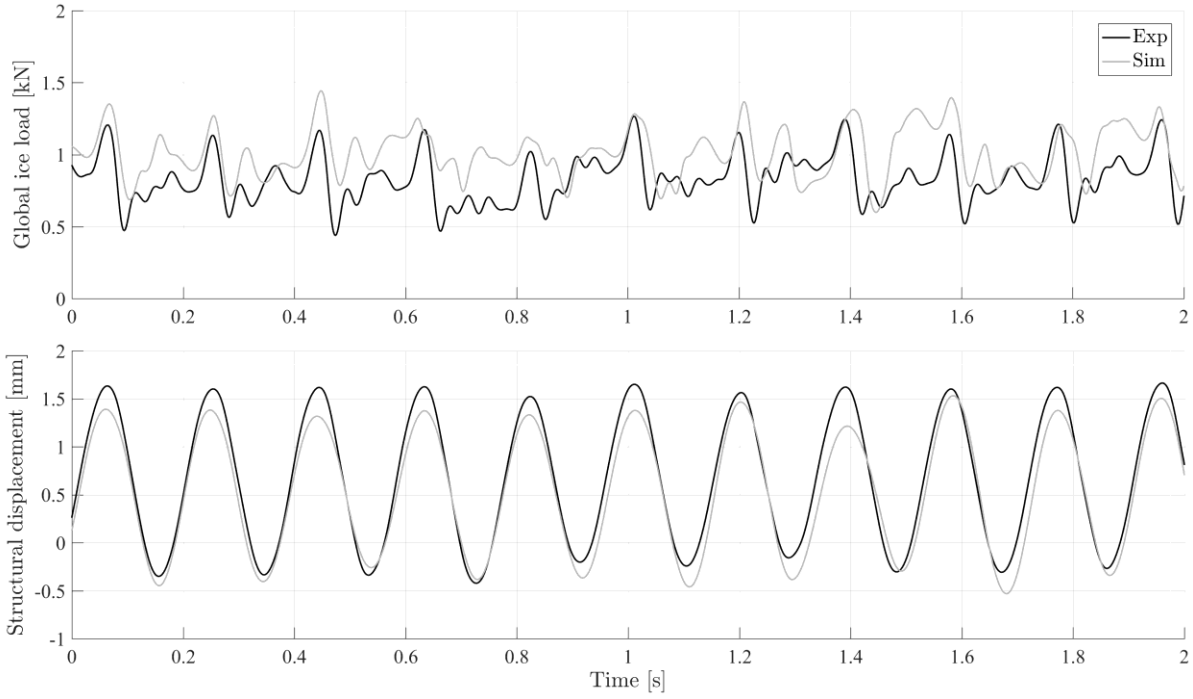

Fig. 4. Comparison of global ice load and structural displacement time traces in the frequency lock-in regime from experimental (Exp) results and simulated (Sim) results with mean ice conditions (trial T9_0) and mean load adjustment at an indentation speed of 0.029 m s^{-1}.

8. Conclusion

Experiments in model ice from Phase 1 and 2 of the IVOS project have been simulated using the analytical model with reference input parameters from a reference structure and accurate predictions of the frequency lock-in regime for each experiment have been shown. Proper estimation of the mean global ice load level in crushing is demonstrated to be very important for accurate prediction of the range of indentation speeds during which frequency lock-in vibrations develop. It is proposed that further research is focused on simulating more experiments with different ice conditions and structures while still utilizing the reference input parameters as determined in Hendrikse et al. (2018). Moreover, the experiments should comprise ice-structure interaction during which the ice fails only in crushing.

Acknowledgements

The authors gratefully acknowledge the support from the SAMCoT CRI through the Research Council of Norway and all of the SAMCoT partners. In particular, the authors wish to thank partners involved in the IVOS project: DNV GL, Engie SA, Kvaerner AS, Multiconsult AS, Shell Technology Norway AS, Total E&P Norge AS, and project coordinator HSVA.

References

Hendrikse, H. (2017). Ice-induced vibrations of vertically sided offshore structures. PhD Dissertation, Delft University of Technology, Faculty of Civil Engineering and Geosciences, Delft.

Hendrikse, H., Ziemer, G., and Owen, C. C. (2018). Experimental validation of a model for prediction of dynamic ice-structure interaction. Cold Regions Science and Technology, 1-63.

Hinse, P., Müller, F., and Ziemer, G. (2017). IVOS Progress Report: April 2017. Hamburg: HSVA.

Jeong, S. and Baddour, N. (2010). Comparison of characteristic failure frequency models for ice induced vibrations. JP Journal of Solids and Structures, 4(3):115–137.

Kärnä, T., Andersen, H., Gürtner, A., Metrikine, A., Sodhi, D. S., Loo, M., Kuiper, G., Gibson, R., Fenz, D., Muggeridge, K., Wallenburg, C., Wu, J.-F., and Jefferies, M. G. (2013). Ice-induced vibrations of offshore structures - looking beyond ISO 19906. In Proceedings of the 22nd International Conference on Port and Ocean Engineering under Arctic Conditions, page 12, Helsinki, Finland.

Korzhavin, K. (1971). Action of ice on engineering structures. (U. A. Technical Report Translation TL260, Trans.)

Muhonen, A. (1996). Evaluation of three ice-structure interaction models. PhD thesis, Helsinki University of Technology.

Owen, C. C. (2017). Ice-induced vibrations of vertically sided model structures: Comparison of structures with circular and rectangular cross-section subjected to the frequency lock-in regime. Delft University of Technology. Delft: Delft University of Technology.

Yu, W., and Blanchard, J. P. (1996). An elastic-plastic indentation model and its solutions. Journal of Materials Research, 11(9), 2358-2367.

Ziemer, G., and Hinse, P. (2017). Relation of maximum structural velocity and ice drift speed during frequency lock-in. Port and Ocean Engineering under Arctic Conditions, (pp. 1-12). Busan.